Influence of imperfections on the photonic insulating and guiding properties of finite Si-inverted opal crystals

Lavrinenko, Andrei; Wohlleben, Wendel; Leyrer, Reinhold J.

Published in:
Optics Express

Link to article, DOI:
10.1364/OE.17.000747

Publication date:
2009

Document Version
Publisher's PDF, also known as Version of record

Influence of imperfections on the photonic insulating and guiding properties of finite Si-inverted opal crystals

Andrei V. Lavrinenko,[1*] Wendel Wohlleben[2] and Reinhold J. Leyrer[2]

[1]*DTU Fotonik, Technical University of Denmark, 2800 Kgs. Lyngby, Denmark*
[2]*Polymer Research, BASF SE, 67056 Ludwigshafen, Germany*
**Corresponding author: alav@fotonik.dtu.dk*

Abstract: The stability of the photonic properties of Si-infiltrated opals for fabrication disorder is tested with following models of applied imperfections: deviations in radii of spheres, deviations in spheres positions and both of them. The deviations are assumed to be distributed accordingly to the normal law and to the skewed distribution experimentally observed in the process of production of polymer self-assembled crystals. The criteria for the photonic crystals tolerances are evaluated versus the quality of photonic insulation provided by films or bulk spheres of finite thicknesses. In addition the stability of the photonic crystal waveguides in inverted opals is tested versus the imperfections strength.

OCIS codes: (050.6875) Three-dimensional fabrication; (130.5296) Photonic crystal waveguides; (160.5298) Photonic crystals

References and Links

1. S. A. Rinne, F. Garcia-Santamaria, and P. V. Braun, "Embedded cavities and waveguides in three-dimensional silicon photonic crystals," Nature Photon. **3**, 2222-2226 (2008).
2. Y. Nishijima, K. Ueno, S. Juodkazis, V. Mizeikis, H. Misawa, T. Tanimura, and K. Maeda, "Inverse silica opal photonic crystals for optical sensing applications," Opt. Express **15**, 12979-12988 (2007).
3. M. A. Kaliteevski, J. Manzaranes Martinez, D. Cassagne, and J. P. Albert, "Disorder-induced modification of the transmission of light in a two-dimensional photonic crystal," Phys. Rev. B **66**, 113101 (2002)
4. M. L. Povinelli, S. G. Johnson, E. Lidorkis, and J. D. Joannopoulos, "Effect of a photonic band gap on scattering from waveguide disorder," Appl. Phys. Lett. **84**, 3639-3641 (2004).
5. D. Gerace and L. C. Andreani, "Disorder-induced losses in photonic crystal waveguides with line defects," Opt. Lett. **29**, 1897-1899 (2004).
6. O. Kilic, S. Kim, W. Suh, Y.-A. Peter, A. S. Sudbø, M. F. Yanik, S. Fan, and O. Solgaard, "Photonic crystal slabs demonstrating strong broadband suppression of transmission in the presence of disorder," Opt. Lett. **29**, 2782-2784 (2004).
7. M. A. Kaliteevski, D. M. Beggs, S. Brand, R. A. Abram, and V. V. Nikolaev, "Stability of the photonic band gaps in the presence of disorder," Phys. Rev. B **73**, 033106 (2006).
8. R. Ferrini, D. Leuenberger, R. Houdre, H. Benisty, M. Kamp, and A. Forchel, "Disorder-induced losses in planar photonic crystals," Opt. Lett. **31**, 1426-1428 (2006).
9. Yu. A. Vlasov, V. N. Astratov, A. V. Baryshev, A. A. Kaplyanskii, O. Z. Karimov, and M. F Limonov, "Manifestation of intrinsic defets in optical properties of self-organized opal photonic crystals," Phys. Rev. E **61**, 5784-5793 (2000).
10. Z.-Y. Li and Z.-Q. Zhang, "Fragility of photonic band gaps in inverse-opal photonic crystals," Phys. Rev. B **62**, 1516-1519 (2000).
11. V. Yannopapas, N. Stefanou, and A. Modinos, "Effects of stacking faults on the optical properties of inverted opals," Phys. Rev. Lett. **86**, 4811-4814 (2001).
12. V. N. Astratov, A. D. Adawi, S. Fricker, M. S. Skolnick, D. M. Whittaker, and P. N. Pusey, "Interplay of order and disorder in the optical properties of opal photonic crystals," Phys. Rev. B **66**, 165215 (2002).
13. F. Galisteo Lopez and W. L. Vos, "Angle-resolved reflectivity of single-domain photonic crystals: Effects of disorder," Phys. Rev. E **66**, 036616 (2002).
14. A. F. Koenderink and W. L. Vos, "Light exiting from real photonic band gap crystals is diffuse and strongly directional," Phys. Rev. Lett. **91**, 213902 (2003).
15. V. Yannopapas, A. Modinos, and N. Stefanou, "Anderson localization of light in inverted opals," Phys. Rev. B **68**, 193205 (2003).

#104159 - $15.00 USD Received 20 Nov 2008; revised 12 Dec 2008; accepted 13 Dec 2008; published 8 Jan 2009

16. M. Allard and E. H. Sargent, "Impact of polydispersity on light propagation in colloidal photonic crystals," Appl. Phys. Lett. **85**, 5887-5889 (2004).
17. A. F. Koenderink, A. Lagendijk, and W. L. Vos, "Optical extinction due to intrinsic structural variations of photonic crystals," Phys. Rev. B **72**, 153102 (2005).
18. E. Palacios-Lidon, B. H. Juarez, E. Castillo-Martinez, and C. Lopez, "Optical and morphological study of disorder in opals," J. Appl. Phys. **97**, 063502 (2005).
19. R. Rengarajan, D. Mittleman, C. Rich, and V. Colvin, "Effect of disorder on the optical properties of colloidal crystals," Phys. Rev. E **71**, 016615 (2005).
20. W. H. Press, S. A. Teukolsky, W. T. Vetterling, and B. P. Flannery, *Numerical Recipes in FORTRAN* (Cambridge University Press, New York, 1992).
21. A. Blanco and C. López, "Silicon onion-layer nanostructures arranged in three dimensions," Adv. Mater. **18**, 1593-1597 (2006).
22. W. Mächtle and L. Börger, *Analytical Ultracentrifugation of Polymers and Nanoparticles* (Springer, 2006).
23. H. Cölfen, *Analytical Ultracentrifugation of Nanoparticles, in Encyclopedia of Nanoscience and Nanotechnology* (American Scientific Publishers, 2004), p.67-88.
24. C. Kittel, *Introduction to Solid State Physics* (Wiley & Sons, New York, 1971).
25. A. Lavrinenko, P. I. Borel, L. H. Frandsen, M. Thorhauge, A. Harpoth, M. Kristensen, T. Niemi, and H. M. H. Chong, "Comprehensive FDTD modeling of photonic crystal waveguide components," Opt. Express **12**, 234-248 (2004).
26. E. P. Petrov, V. N. Bogomolov, I. I. Kalosha, and S. V. Gaponenko, "Spontaneous emission of organic molecules embedded in a photonic crystal," Phys. Rev. Lett. **81**, 77-80 (1998).
27. K. Busch and S. John, "Photonic band gap formation in certain self-organizing systems," Phys. Rev. E **58**, 3896 (1998).
28. E. Palacios-Lidon , A. Blanco , M. Ibisate, F. Mesequer, J. C. Lopez, and J. Sanchez-Dehesa, "Optical study of the full photonic band gap in silicon inverse opals," Appl. Phys. Lett. **81**, 4925-4927 (2002).
29. A. Chutinan and S. Noda, "Highly confined waveguides and waveguide bends in three-dimensional photonic crystal," Appl. Phys. Lett. **75**, 3739-3941 (1999).
30. M. L. Povinelli , S. G. Johnson, S. Fan, and J. D. Joannopoulos, "Emulation of two-dimensional photonic crystal defect modes in a photonic crystal with a three-dimensional photonic band gap," Phys. Rev. B **64**, 075313 (2001).
31. V. Yannopapas, A. Modinos, and N. Stefanou, "Waveguides of defect chains in photonic crystals," Phys. Rev. B **65**, 235201 (2002).
32. C. Sell, C. Christensen, J. Muehlmeier, G. Tuttle, Z. Y. Li, and K. M. Ho, "Waveguide networks in three-dimensional layer-by-layer photonic crystals," Appl. Phys. Lett. **84**, 4605-4607 (2004).
33. A. Chutinan and S. John, "Diffractionless flow of light in two- and three-dimensional photonic band gap heterostructures: Theory, design rules, and simulations," Phys. Rev. E **71**, 026605 (2005).
34. Y. Jin, C. A. Leatherdale, and D. J. Norris, "Tailoring air defects in self-assembled photonic bandgap crystals," Adv. Mater. **17**, 1908-1911 (2005).
35. V. Lousse, J. Shin, and S. Fan, "Conditions for designing single-mode air-core waveguides in three-dimensional photonic crystals," Appl. Phys. Lett. **89**, 161113 (2006).
36. V. Lousse and S. Fan, "Waveguides in inverted opal photonic crystals," Opt. Express **14**, 866-78 (2006).
37. Y. A. Vlasov, X. Bo, J. C. Sturm, and D. Norris, "On-chip natural assembly of silicon photonic bandgap crystals," Nature **414**, 289-293 (2001).
38. K-C. Kwan, X. Zhang, Z.-Q. Zhang, and C. T. Chan, "Effect due to disorder on photonic crystal-based waveguides," Appl. Phys. Lett. **82**, 4414-4416 (2003).

1. Introduction

Three-dimensional (3D) photonic crystals (PhCs) possessing complete photonic band gaps (PBG) have been aimed for while for effective optoelectronic applications. Compactness and functionality acquired in such devices are fully grounded on the properties of defects like cavities and waveguides engineered in the spatial lattices of periodically distributed elements (spheres, pillars, bars, etc.). So the role of a 3D PBG structure examined as a template for inscription photonic components is twofold: (i) it is a supporting platform, which contains photonic components holding them mechanically in space; (ii) it serves as an effective photonic insulator, providing acceptable level of losses for modes following complex 3D-profiled design of defects. Mechanical stiffness of the platform is a question lying further ahead. Currently, the most fragile for fabrication imperfections are insulating properties.

We believe that the new impulse to activity in this direction has been given recently by Rinne et al [1], who reported on the waveguiding effect of the near-infrared light in silicon inverted opals. The authors managed to overcome processing challenges and fabricated 3D PhCs with reasonable sizes of operational area and showed transmission of light in 2μm x

#104159 - $15.00 USD Received 20 Nov 2008; revised 12 Dec 2008; accepted 13 Dec 2008; published 8 Jan 2009

2μm square channels. Such large air-guiding core might have multimode guidance. In order to achieve single-mode operation of linear defects their cross-section sizes should be inevitably reduced and consequently the effect of fabrication imperfections will be enhanced. Another inverted opals application addressed recently in the literature is sensing [2], which is also very sensitive for disorder. So, the crucial question we are going to address in the paper is to quantify tolerances, which can a silicon inverted opal of finite sizes bear still providing required insulating properties.

In reality there are several sources of structural imperfections: variations in atoms positions, changes in radius and shape, surface roughness, doping of various substances, etc. Here, we would like to analyze the resistance of Si inverted opal platform to possible disorder in arrangement of elements of its spatial lattice and their polydispersity.

Disorder is notorious for causing problems in photonics in regarding opening and holding complete or directional bandgaps. This question is discussed in numerous references addressing models of disorder in 1D-2D lattices [3-8] or in full 3D crystal arrangement [9-19]. The former models are applied to planar PhCs and photonic crystal waveguides (PCWs). The latter references are dealing mostly with face centered cubic (FCC) structures like opals. The most advanced model for the crystal structure with imperfections includes the special rules for minimization of energy to assemble colloidal particles in the densest way during the self-assembling process [16].

Due to fabrication challenges imperfections effect on the photonic properties of silicon inverted opals has been studied only theoretically [10]. The authors tested fragility (or controversy stability) of the PBGs in silicon inverted opals against positions (sites) and radius (sizes) imperfections with homogeneous statistical distribution. Conclusion made after the performed analysis imposes strict constraints on the fabrication tolerances. For example, 5% variations in radius and holes positions close the PBG in an infinite structure, thus posing the first crude constrain on the fabrication tolerances. However, this constrain should be toughened for real structures taking into account their finite sizes and other kinds of imperfection distributions. However, as PhCs are considered for providing insulating effect only, the severe restrictions imposed on the quality of PhCs serving for photonic circuits (polydispersity < 0.25% [14]) can be softened, leading us to more or less reasonable technical numbers for spheres polydispersity.

The paper is organized as follows. Section 2 describes the models of imperfection used and the layout of the numerical experiment. In Section 3 results of numerical experiments on photonic insulation with two statistical models of imperfections are given. The finite-difference time-domain method (FDTD) is employed to characterize effect of imperfections on the photonic insulation. Effect of disorder on guiding properties of hollow defects in Si inverted opals is studied in Section 4. Finally, conclusions are summarized in Section 5.

2. Models of imperfections

As it has been thoroughly described in literature there are several fabrication steps in producing silicon inverted opals. In practice, imperfections occur at every step of the fabrication process. Among possible imperfections we picked up two of them: deviations in sizes of spheres (radius or diameter deviations) and variations in their positions (sites deviations). Such choice of imperfections has been discussed previously [10]. Distribution of imperfections is assumed to be Gaussian, which is in contrary to the previous case [10], but actually close to the real one (see below).

We utilize procedure described in Press et al. [20] to transform a series of random numbers generated by the pseudorandom generator of a FORTRAN compiler homogeneously distributed on the unit interval into a series with the distribution accordingly to the Gaussian law. The procedure can be easily extended beyond the unit interval. Let x_1 and x_2 be two sets of independent uniformly distributed pseudorandom numbers on unitary interval. Then transformation

$$y_1 = \sigma\sqrt{-\ln x_1}\cos 2\pi x_2, \quad y_2 = \sigma\sqrt{-\ln x_1}\sin 2\pi x_2 \tag{1}$$

#104159 - $15.00 USD Received 20 Nov 2008; revised 12 Dec 2008; accepted 13 Dec 2008; published 8 Jan 2009

leads to two independent deviates y_1 and y_2 with the normal differential distribution characterized by one dimensionless parameter - a standard deviation σ:

$$p(y)dy = \frac{1}{\sqrt{2\pi}\sigma}\exp\left(-\frac{y^2}{2\sigma^2}\right)dy\,. \tag{2}$$

These two sets of numbers are employed to impose randomization on radii and coordinates of all spheres constituting a piece of inverted opal structure. The natural choice for the scaling factor is $r_0 = 0.353553a$ - the radius of rigid spheres in cubic close packed (ccp) arrangement normalized to the lattice constant a [10]. New randomize coordinates of spheres centers and their radius designated in general case by F_r are expressed through a random number y as

$$F_r = F_0 + yr_0 \tag{3}.$$

Here variable F_0 stands for the regular (perfect) values of the corresponding variable.

We checked the randomization procedure by applying 100 000 single precision realizations with $\sigma = 0.05$. The standard deviation of the distribution estimated externally (by utilities of the *Mathematica* package) is 0.0501414, while the mean value equals 0.000187303. Thus we conclude that our randomization procedure is sufficiently accurate (in the 4th digit) for the imperfection modeling.

The Gaussian distribution of imperfections is not the only one we used. Polymer opal templates are considered as a competitive alternative to the artificial glass opals featuring an inversion process [21]. Imperfections produced during the template self-assembling from the colloids trigger all other possible disorders in the technological chain. Strikingly, polymer spheres polydispersity measured in solution reveals quite different statistical behavior.

Polymer spheres size dispersion was characterized in solution with the analytical ultracentrifugation [22] (AUC). AUC is a fractionating technique such that – in contrast to light scattering – a distribution of sizes is determined with high resolution. Furthermore – in contrast to electronic microscopy – the AUC integrates over 10^9 – 10^{12} particles, such that statistical relevance even of minor fractions is high. In a sedimentation field ramp from 600 rpm to 40 000 rpm (acceleration of up to 150 000g), solutes and nanoparticles from primary to agglomerates sediment in fractions that are separated according to their size in the range 20 – 3000 nm. Simultaneous detection by synchronized optics quantifies the amount and the diameter of each fraction independently [23]. Note that the AUCs used here are home-build with a number of features (no gradients, no discs, correction of dilution and scattering effects) that further enhance the resolution and accuracy compared to the commercially available AUCs from Brookhaven or CP Instruments. Our AUCs are based on Beckman models XL and have been modified for the online recording of sedimentation with turbidity, Schlieren, interference, absorption and X-Ray detection [22]. Turbidity optics, recording the gradual increase of laser transmission over time $I(t)$, is the most suitable for polymer sphere analysis. In order to convert the observed distribution of sedimentation constants s to diameters d, we rely on the simplifications of the Stokes-Einstein relation:

$$d = \sqrt{\frac{18\eta s}{\Delta\rho}}\,, \tag{4}$$

where η is the viscosity of the solvent (η = 0.893 g/m/s for water), and $\Delta\rho$ is the density difference between the solute and the solvent ($\Delta\rho$ = 0,057 g/cm³ for polystyrene at 25°C). In order to extract the actual size distribution from the intensity-weighted signal heights in the raw transmission / time $I(t)$ data, the evaluation takes full account of dynamic dilution effects and the Mie scattering [22]. The integral distribution can be differentiated to give the peak presentation of size distribution.

We find that the actual distribution of polymer dispersions is not symmetrical but skewed with more coarse than fine fraction, see the differential distribution in Fig.1. We will refer hereafter to this distribution as the skewed distribution. Mean standard deviation is hence not an optimal measure of polydispersity, but can be used for comparison. In addition to the

#104159 - $15.00 USD Received 20 Nov 2008; revised 12 Dec 2008; accepted 13 Dec 2008; published 8 Jan 2009

standard deviation parameter we introduce the polydispersity index $PI = \left(D_{90} - D_{10} \middle/ D_{50} \right)$ due to its higher sensitivity to detrimental coarse fraction than the usual standard deviation of particle size. All present samples achieve $PI = 0.08 - 0.09$. Additional experiments were performed to quantify the polydispersity of the spheres that are actually assembled into the opal. To that aim, we tried to dissolve the polymer opal by ultrasound and surfactants. However, the spheres could not be fully separated again, such that a remaining fraction of dimer and trimer obscured the determination of a *PI* after self-assembly. We hence rely on the assumption that all spheres are incorporated into the opal regardless of small size variations, such that the polydispersity inside the opal is the same as before self-assembly.

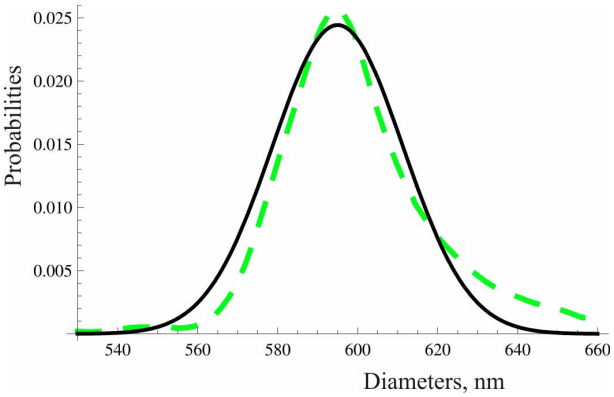

Fig. 1. The dashed green curve: the differential size distribution of polymer spheres from analytical ultracentrifugation, integrating over ~10^9 particles in the original diluted suspension. The black solid curve: the best normal fit ($\sigma \approx 0.02$) to the skewed distribution

By the use of the integral distribution provided by the AUC method, we mimicked polydispersity of the spheres radii naturally occurred in the fabrication process. The first trial consists of 100 000 random numbers generated by a FORTRAN code accordingly to the provided statistics. All numbers are distributed in 147 bins. The envelope resembles measured data distribution with some flashes of nonmonotonic behavior. The structures used in numerical experiments are certainly less populated. For example, in transmission analysis a 15-layers inverted opal film is exploited. It consists of 930 spheres, so differential distribution approximated by dividing all numbers into 147 bins appears to be locally nonmonotonic (Fig.2). Of course, we expect that visual similarity of modeled and real distributions will be more and more accurate with the increase of number of generated random values. For the final proof we validated our simulation procedure by direct comparison of both integral distributions (see inset Fig. 2), which unambiguously shows their similarity in spite of the small number of realizations (930) in the numerical procedure. The best Gaussian fit to the skewed distribution has the standard deviation $\sigma \approx 0.02$, see the solid curve black curve in Fig.1. It will be used below as a reference.

#104159 - $15.00 USD Received 20 Nov 2008; revised 12 Dec 2008; accepted 13 Dec 2008; published 8 Jan 2009

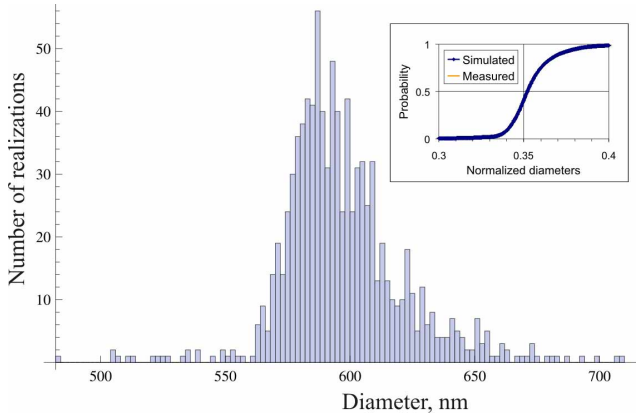

Fig. 2. The skewed distribution realized by 930 random numbers generated by the FORTRAN program and divided into 147 bins. Inset shows comparison of the skewed and simulated integral distributions.

3. Effect of imperfections on photonic insulation

3.1 Imperfections influence on transmission spectra

To check the influence of imperfections on photonic properties of inverted opals we performed first a set of numerical exercises with transmission, which have straightforward laboratory analogues. Thin films are constructed from (111) planes arranged in the ABC sequence [24], so that the film is oriented in the most common in experiments principle direction of the FCC lattice. The thickness of the film is 15 layers. We will refer to it as the 5ABC *Γ-L* film. The structure's transmission is revealed after averaging over spectra FDTD calculated (see details elsewhere [25]) with 7 different statistical realizations of the correspondent disorder for each set of parameters.

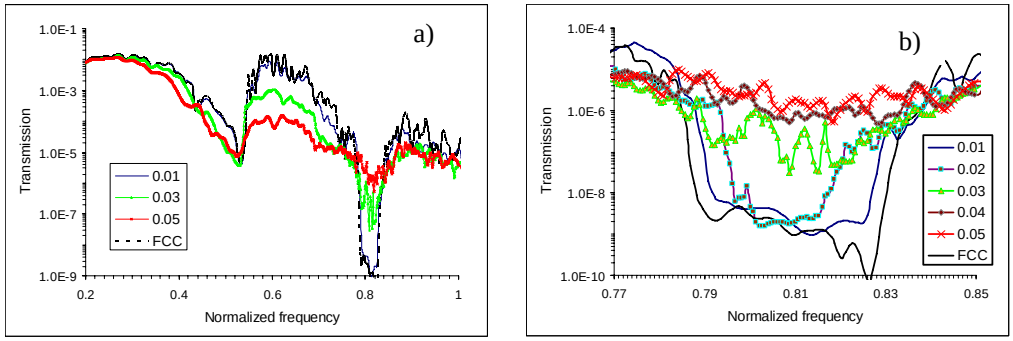

Fig. 3. Averaged transmission spectra in *Γ- L* direction for 15 layers of Si inverted opal with deviations in radius. Mean standard deviations of radius imperfections are shown in the specification table. Transmission spectrum for the sample with the perfect FCC lattice is shown by the black line; (b): zooming in the PBG region.

Transformation of the transmission spectra for the 5ABC Γ-L silicon (refractive index n = 3.476) inverted opal film in the presence of radius imperfections is shown in Fig. 3(a). Frequency here and throughout the paper is presented in the normalized units $f = a/\lambda$. As it can be anticipated the low frequency part of the transmission curve is almost unaffected by the imperfections due to the validity of the effective medium approximation. The most affected by the radius imperfections is the PBG zone. It is zoomed in for better visualization in Fig. 3(b). Disorder deteriorates photonic insulation lifting up transmission in the PBG range, thus,

#104159 - $15.00 USD Received 20 Nov 2008; revised 12 Dec 2008; accepted 13 Dec 2008; published 8 Jan 2009

signaling about the PBG closing. For reference we use transmission spectrum for the perfect film shown by the black line. The depth of the PBG, which defines the strength of photonic insulation, can be roughly estimated in 50 dB (for 15 layers only!). However, radius imperfections with mean standard deviation σ = 0.03 significantly reduced the transmission gap in width and in depth hampering to achieve appropriate photonic insulation. Standard deviation σ = 0.04 practically diminishes the PBG.

The similar results occur with cites imperfections, by which we mean deviations of positions of spheres from their fixed arrangement in the FCC lattice. The Gaussian distribution is applied independently for each of the Cartesian coordinates of the spheres centers through formula (3). Eventually, spheres radii and positions of the centers are randomized independently with the normal distribution. We designate them accordingly by "*s&s*" sign (sizes and sites) as adopted in Li and Zhang [10]. Significant shrinkage of the PBG sizes is observable for imperfections distributed normally with σ = 0.02. The PBG effect (insulation) is completely vanished with σ = 0.03 imperfections. So in comparison with results acquired for the infinite structures (closing of band gaps with σ = 0.04 imperfections in sites and sizes [10] this means that stricter constrains on the fabrication quality for real, i.e. finite, systems should be imposed.

We also aimed to test the rule certified for infinite structures [10] that the PBG is more sensitive to radii than sites imperfections. FDTD calculated transmission spectra are configured for such comparison together with the transmission of the perfect lattice in Fig. 4. So, for the reasonable disorder (σ = 0.03 and less) constrains are tougher for radii imperfections, see Fig. 4(a). For intensive disorder (standard deviation σ = 0.05), structures with radii imperfections exhibit a bit better results (Fig. 4(b)). Nevertheless, it is difficult to judge in such way, because the PBG effect is ruined anyway.

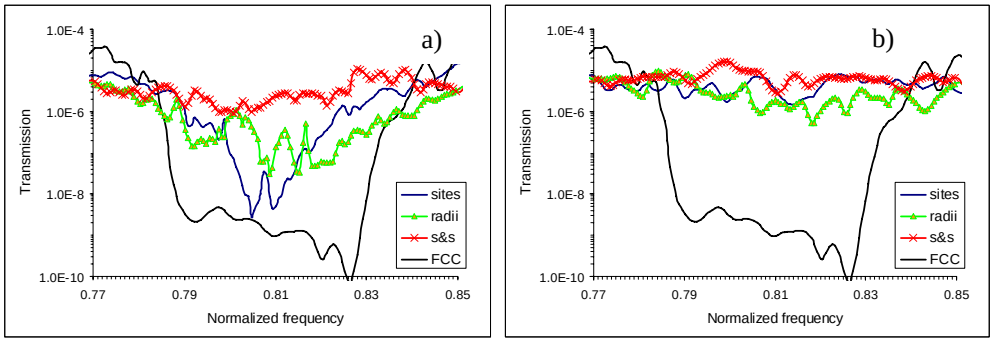

Fig. 4. Averaged transmission spectra in Γ- L direction for 15 layers of Si inverted opal with deviations in spheres positions and/or radii: (a) σ = 0.03, (b) σ = 0.05. Transmission spectrum for the sample with the perfect FCC lattice is shown by the black line

Implementation of the second model of imperfections, namely the skewed distribution, provided striking result. For better comparison we put together on the same chart transmission through the 15-layers Γ-L sample with different types of imperfections: radius imperfections under the skewed distribution and both radius-site imperfections accordingly to the Gaussian law (Fig. 5). The designation, for example, "r = 0.02" means that imperfections in the spheres radii obey the normal distribution with the mean standard deviation σ = 0.02. Results unambiguously certify that the skewed distribution produces much more damage on the photonic insulation than the closest Gaussian fit for radius imperfections with σ = 0.02 and even size-and-sites disorder with σ = 0.03. This fact puts tougher constrains on the fabrication tolerances and should be taken into account in technological issues.

#104159 - $15.00 USD Received 20 Nov 2008; revised 12 Dec 2008; accepted 13 Dec 2008; published 8 Jan 2009

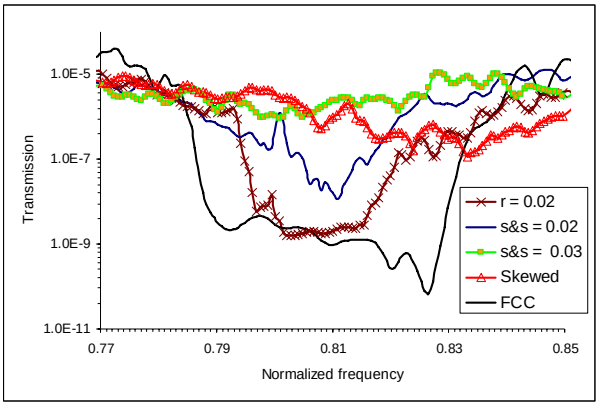

Fig. 5. Averaged transmission spectra in Γ- L direction for 15 layers of Si inverted opal with deviations in spheres positions and radii. Mean standard deviations of coordinate and radii imperfections are shown in the specification table Transmission spectrum for perfect PhC is shown in black.

3.2 Direct proof of tolerances for photonic insulation

In Subsection 3.1 we analyzed the influence of imperfections on transmission of light through a thin film of the inverted opal. In spite of that results seem to be reasonable they cannot be used as a comprehensive proof neither of existence nor of ruining of the complete PBG in finite photonic crystals with imperfections. Actually, what we proved by transmission simulations, is that the directional Γ- L bandgap is gradually closing as a result of introduced imperfections. Meanwhile, the meaning of the "photonic insulation" guarantees omnidirectional suppression of light propagation. So, in this subsection we focus on another approach attempting to answer the question: how large can be imperfections providing still essential photonic insulation by the inverted opal. The idea of our modeling resembles experiments with the suppression of fluorescence of dye molecules embedded in a PhC possessing a stop band [26]. It is realized it in the following way. We take a big sphere made of Si inverted opal (Fig. 6). The diameter of the sphere is 10a. In the centre of the sphere we insert a broad-band point source consisting of two dipoles of mutually orthogonal polarizations. A set of point detectors is placed at the same distance from the centre (next to the surface), but in different directions seen from the centre (see Fig. 6).

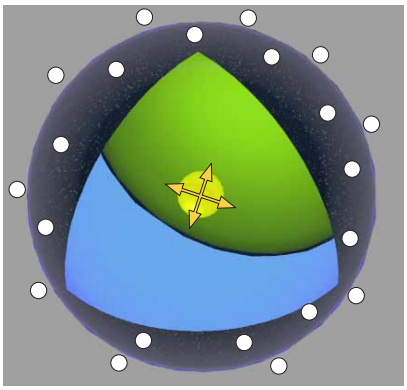

Fig. 6. Layout of the calculation scheme. The sphere from inverted opal is 10a in diameter. A point source consisting of two orthogonal dipoles is in the center. White circles symbolize detectors.

#104159 - $15.00 USD Received 20 Nov 2008; revised 12 Dec 2008; accepted 13 Dec 2008; published 8 Jan 2009

There are three options: randomly placed detectors (1000 points); detectors homogeneously covering the surface (184 points) and detectors arranged in the principal highly symmetrical spatial directions of the FCC lattice seen from the centre of the sphere. There are 6 such points in *Γ-X* (100) directions, 8 in *Γ-L* (111), 12 in *Γ-K* (110) and 24 in *Γ-W* (210). The processing of information stored by detectors includes the Fourier transform of the fields in the frequency domain, averaging the detected signal intensity over the each group of detectors and normalizing data by the number of detectors. Obtained information is a comprehensive check of insulating properties of the material implied in certain directions of particular interest or in all directions simultaneously.

Two examples of the emerged fields intensities for inverted opals made from TiO_2 (n = 2.7), and Si are shown in Fig. 7. Titania inverted opal cannot provide any reasonable photonic insulation as it was anticipated due to the lack of a complete PBG (Fig. 7(a)). It is well known that for the inverted opal structure the PBG is opened from n = 2.9 [27]. The sharp dip in the spectra fixed in all directions is presented in spectra for the Si inverted opal, see Fig. 7(b). The wide and deep ravine 30-40 dB in depth at frequencies between 0.78 and 0.82 reflects perfect photonic insulation by the complete PBG in spite of rather compact dimensions of the protecting shield. From the point of view of directional protection the Γ-W direction has relatively less insulating strength. This result is expected having in mind that the PBG is the narrowest here [27, 28].

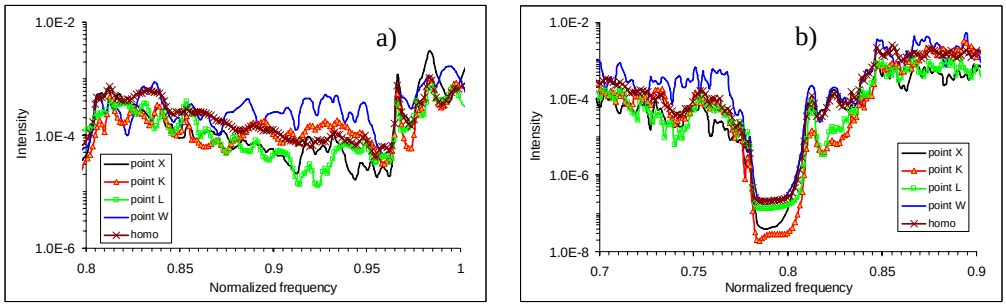

Fig. 7. Normalized intensity spectra for fields emerged from the inverted opal sphere of radius $r = 5a$ in four highly symmetric directions and for homogeneously distributed detectors, for details see specification table in the charts: (a) titania (n = 2.7); (b) (silicon n = 3.476).

The next step is to follow up the collapsing of PBG protection properties as imperfections are introduced in the sphere design. We apply radius and size-and-site randomization with the normal distribution of fluctuations and the skewed distribution of radius fluctuations. First of all, even small uncertainties in the radii and spheres positions of spheres (σ = 0.01) perturb insulation properties of the photonic shield from the silicon inverted opal. Further grow of imperfections strength to the current state-of-the-art (σ = 0.02) [17] severely distorts PBG properties (Fig. 8). Effectively, protection properties of the 5 lattice constant thick layer of the silicon inverted opal disappear when the standard deviation in sites-and-sizes $\sigma \geq 0.03$. Radius imperfections only have a little bit weakened effect on the PBG annihilation. As for directional analysis, the negative influence of disorder is more pronounced in the Γ-W direction, see Fig. 8(d). We also performed evaluation of radius deviations effect on photonic insulation of inverted opals, when randomization obeys the skewed distribution. Yields of modeling are shown in Fig. 8 as well. It is clearly much worse in consequences than imperfections distributed by the nearest normal fit (σ = 0.02).

It should be mentioned that our evaluations are based on the numerical realization of the FCC lattice in the FDTD method. However, due to the staircase approximation used to place spheres onto the square grid, small deviations in spheres positions and radii within the close packing lead to the background level of imperfections presented even in the perfect case. So, our results in tolerances frames might be moderated. One more consequence of the staircase

#104159 - $15.00 USD Received 20 Nov 2008; revised 12 Dec 2008; accepted 13 Dec 2008; published 8 Jan 2009

approximation is the overestimating of the air fill of the inverted system, which results in little blue shift of the bands.

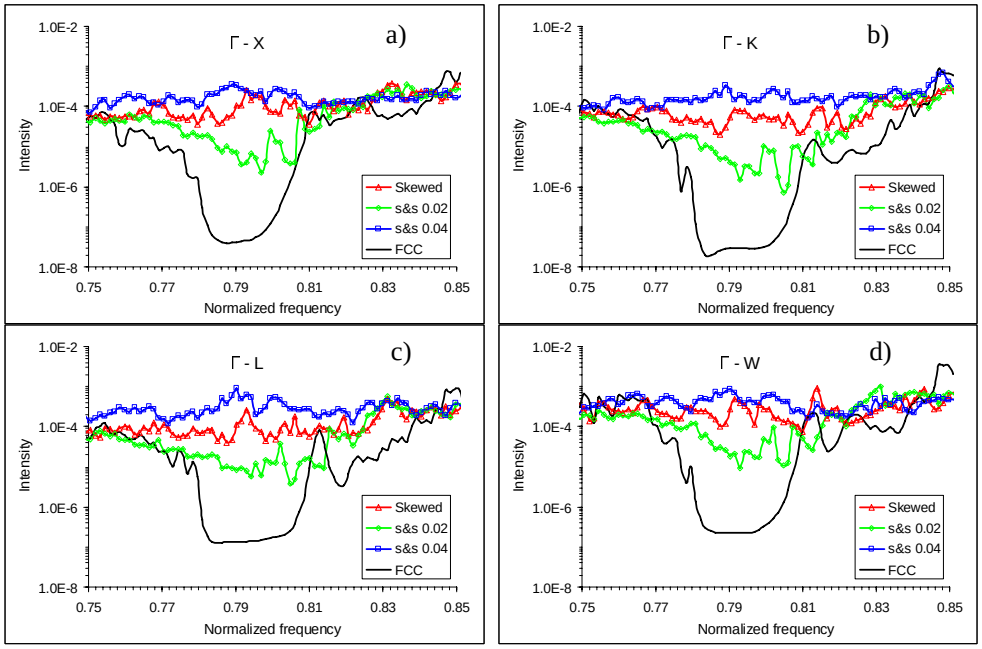

Fig. 8. Normalized intensity spectra for fields emerged from the inverted opal sphere with the normal distribution of s&s deviations and the skewed distribution of radii, see the specification tables for details, a) in *Γ-X* direction; b) in *Γ-K* direction, c) in *Γ-L* direction; d) in *Γ-W* direction. The spectra for the perfect PhC in correspondent direction are shown in black lines.

4. Effect of imperfections on properties of waveguides in 3D photonic crystals

Currently, one of the main targets is to investigate possibility of effective light transport in waveguides embedded as line defects in a photonic crystal template exploiting the properties of the complete PBG. Different designs have been proposed and modeled, some of them have been fabricated and characterized [1, 29-36]. Here we are interested in tolerances to disorder of waveguides inscribed in inverted opals templates. Procedure of calculation is set up in the following way. A spatial distribution of electric and magnetic field vectors at zero time moment is defined closely to the input entrance of a PCW emulating a broadband impulse. This impulse is impinging on the interface of a PhC block travelling some distance in air before to produce a Maxwellian propagating field. Detectors and all geometrical sizes are kept the same as in the case of the perfect FCC arrangements, so any comparisons between, e.g. transmission spectra with and without defect, can be made in an accurate way. All calculations are repeated in the same configuration of the layout but in air to provide reference data.

4.1 Waveguides in inverted opal structure

Due to the complex spatial symmetry of the FCC lattice there are a lot of variants how to choose directions of the inscribed waveguide in the bulk crystal. Principally there should be several directions in order to provide some functionality with photonic contours. To simplify our task we choose 3 principle directions for guiding light through: *Γ-X*, *Γ-K* and *Γ-L*. Waveguides are defined as a straight channels inscribed in inverted opal films perpendicular to corresponding symmetric planes: (100) for *Γ-X*, (110) for *Γ-K* and (111) for *Γ-L* channels. Two basic shapes of PCWs are considered: cylindrical and as a chain of spheres [36]. A cylindrical photonic crystal waveguide (CPCW) is made as a straight cylindrical air defect

#104159 - $15.00 USD Received 20 Nov 2008; revised 12 Dec 2008; accepted 13 Dec 2008; published 8 Jan 2009

inserted in an inverted opal structure. A chain of spheres (CoS) is made of spheres, whose centers are positioned on the same line with periodicity reflecting directional FCC lattice planes repetition. Apart from the spatial orientation of the waveguide, there are, at least theoretically, several possibilities to center a guiding channel in each of the films stemming from the in-plane symmetrical properties. To keep the symmetry of the structure as high as possible we limited ourselves with few symmetrical points. For example, we tried three different positions of waveguide input for Γ-X, 4 for Γ-K and 4 for Γ-L PCWs. Results in transmission differ significantly, resembling the strong dependence of transmission properties not only on direction, but on waveguides position.

For methodological purposes we first show the raw data of one of the CPCW transmission simulations (Γ-K CPCW, $r = 0.354a$), see blue curve in Fig. 9. The absolute level of transmission, which is about -20 dB, is not informative enough, because it includes losses for coupling of light emitted by the highly divergent source to the waveguide modes. For clarity the perfect FCC spectrum is provided (the black curve in Fig. 9). It shows the PBG position around normalized frequency $a/\lambda = 0.8$. It is obvious that enhanced transmission exceeding the average level by approximately 10 dB is observed exactly in the PBG region. To elaborate reasonable criteria for evaluation of the waveguides properties we calculate transmission detected by the same disposition of the sources and detectors but in air (red curve with squares in Fig. 9). Thus, in what follows we present spectral dependencies of transmission through PCWs normalized to the transmission in air. Our goal is to investigate how tolerant to imperfections are transmission peaks for modes guided in the PBG zone. The most interesting are peaks, which extend significantly over the reference level given by the reference transmission in air.

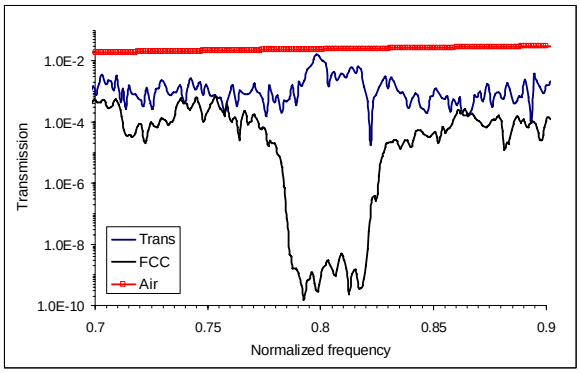

Fig. 9. Transmission through Γ-K CPCW, $r = 0.354a$ (blue curve), perfect PhC (black curve) and in the same set up in air (red line with squares).

From the all variety of transmission curves we chose the cases providing the best performance for waveguides. There are: in the Γ-K film, CPCW with radius $r = 0.45a$ and CoS with $r = 0.48a$, both centered between the rows of spheres; in the Γ-X film, CPCW with $r = 0.45a$ centered between the touching spheres and CoS, $r = 0.5a$ centered in the gap between four neighboring spheres; in the Γ-L film, CPCW, $r = 0.42a$ just in the center of a sphere and CoS, $r = 0.55a$ in the gap between three neighboring spheres. As one can conclude from this nomenclature, the Γ-K CoS waveguide with $r = 0.45a$ does not obtain the highest transmission level in spite of the widest single mode guided band [36].

4.2 Transmission in waveguides with imperfections

We begin with waveguides in the Γ- K films. The absolute level of transmission with the peak value about 0.23, as we mention above, has limited significance, because of interplay of several factors hampering transmission of light through waveguides: coupling, detection, etc, which are difficult to trace out. In other words, there are no any distinct and universal

#104159 - $15.00 USD Received 20 Nov 2008; revised 12 Dec 2008; accepted 13 Dec 2008; published 8 Jan 2009

references to judge about efficiency of transmission properties of PCWs besides the comparative level of transmission detected by the same layout, but in air. Normalized transmission around 1.0 should be treated as unacceptably low.

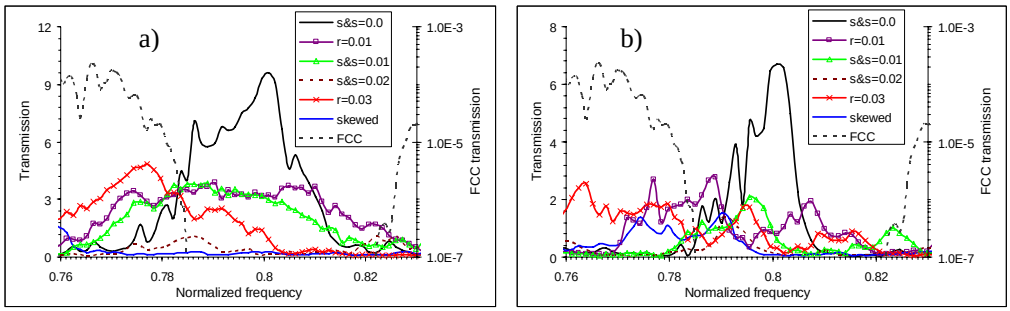

Fig. 10. Normalized transmission spectra for Γ- K waveguides with deviations in radii and positions of spheres. Mean standard deviations and types of imperfections are shown in the table. Transmission spectra for the undistorted waveguides are shown by the solid black line (s&s=0.0); transmission of the perfect FCC sample is marked by the dashed black line. a) CPCW (r = 0.45a, thickness 7.1a); b) CoS (r = 0.49a, thickness 7.1a)

Transmission spectra of CPCWs (r = 0.45a) with and without imperfections normalized in the way described above are presented in Fig. 10(a). The broad passband, extended over the bigger part of the PBG, is a clear signature of the transmission in the Γ- K films. Deviations in radii (r-imperfections) and in both radii and positions (s&s-imperfections) of spheres as small as σ = 0.01 reduce transmission in 2-3 times across the whole band. Further growth of imperfections eradicates any abilities of bands in the PBG zone to carry on some light throughout the structure, see, e.g. curves r = 0.03 and *s&s* = 0.02. The skewed distribution is the worst, see Fig. 10(a), the blue line. However, there is another characteristic feature of the waveguides in crystals with disorder: instead of noticeable transmission in the PBG zone due to the light confinement in the air channel by the mirror properties of a 3D photonic crystal, transmission peaks appear at the edges or even outside the PBG region. See, for example, the peak at frequency 0.774 for r = 0.03, see Fig. 10(a). Such behavior can be attributed to the intensive surface modes originated on the waveguides surface after enhanced corrugation. The role of such modes is mostly negative, because the energy coupled to them will be dissipated on irregularities and can be coupled out with difficulties. We believe that the increment of the waveguide's length will lead to the rapid decrease of these transmission peaks.

The similar picture happens with the CoS waveguide in the Γ- K direction (r = 0.49a), see Fig. 10(b). Here, collapsing of the transmission band in the PBG in presence of imperfections is even faster: about 4 times reduction in transmission for *s&s* = 0.01 imperfections. Peaks beyond the PBG zone are also presented here, see the plateau between 0.76 and 0.78 for r = 0.03, or various peaks for r = 0.01 case.

The next direction of light guiding is Γ- L, that is, the direction through the naturally assembling opal films. The Γ- L film consists of 15 layers (the 5ABC sample). Transmission spectra for CPCW (r = 0.42a) are spiky revealing the multiband character of inscribed defects (Fig. 11(a)). The highest transmission peak at 0.795 is quickly diminished by the growth of radius deviations. However, behavior of defect peaks appeared due to disorder is different from that of the Γ- K case. Apart from the peaks beyond the PBG, transmission in the center of the PBG is even ameliorated by the small imperfections (transmission plateau at 0.80 – 0.81, see Fig. 11(a)). Another result is that the s&s imperfection model, but not the skewed one, leads to the worst changes in transmission (Fig. 11(a)). In overall, CPCWs in Γ- L directions exhibit high sensitivity to the imperfections too.

#104159 - $15.00 USD Received 20 Nov 2008; revised 12 Dec 2008; accepted 13 Dec 2008; published 8 Jan 2009

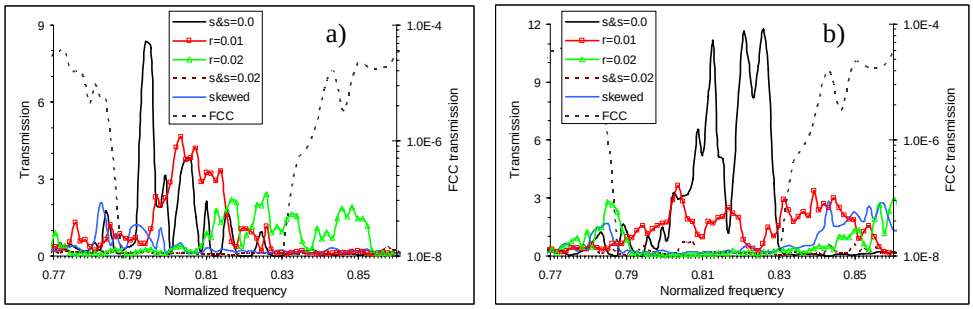

Fig. 11. Normalized transmission spectra for Γ- L waveguides with deviations in radii and positions of spheres. Mean standard deviations and types of imperfections are shown in the table. Transmission spectra for the undistorted waveguides are shown by the solid black line (s&s=0.0); transmission of the perfect FCC sample is marked by the dashed black line. a) CPCW (r = 0.42a, thickness 15 layers); b) CoS (r = 0.55a, thickness 15 layers)

Something similar is observed in evolution of the CoS (r = 0.55a) transmission spectra shown in Fig. 11(b). Defect modes due to disorder are originated in the center of the PBG zone and in the high frequency region outside the PBG. The quantified evaluation of changes is not obvious due to the multiple hops of the bands in the defect structure, nevertheless, the clear message here is that such waveguides are more sensitive to imperfection than Γ- K, namely because of the irregular switching between multiple bands.

Waveguides in Γ- X direction can be regarded as exotic: the (001) planes are not very often observed in opal crystals, so special procedures like cleaving, cracking or sawing were used to obtain the (001) and (011) interfaces [9, 28, 37]. Nevertheless, the progress in the technology of waveguides inserting in the bulk of inverted opals [1] makes the analysis of disorder influence on properties of such waveguide relevant. The CPCW with r = 0.45a, thickness 10a exhibit the highest normalized transmission among all examples we have tested so far. Unfortunately, its remarkable guiding properties are severely distorted by imperfections (Fig. 12). The level of these distortions can be quantified accordingly to data presented in the figure. Some resistivity to the imperfection is exhibited by the mode centered on 0.782 at the PBG edge. Alternative passbands appear now in the long-wave zone beyond the stopzone, in frequency interval 0.76-0.77.

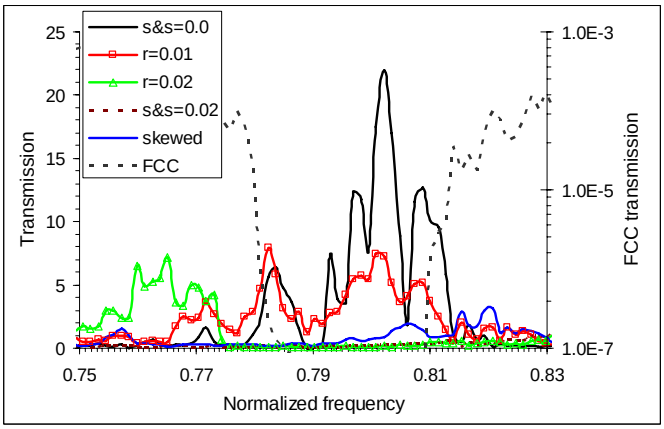

Fig. 12. Normalized transmission spectra for the Γ- X CPCW (r = 0.45a, thickness 10a) with deviations in radii and positions of spheres. Mean standard deviations and types of imperfections are shown in the table. Transmission spectra for the undistorted waveguides are shown by the solid black line (s&s=0.0); transmission of the perfect FCC sample is marked by the dashed black line.

#104159 - $15.00 USD Received 20 Nov 2008; revised 12 Dec 2008; accepted 13 Dec 2008; published 8 Jan 2009

The important remark is that the CoS design shows very low transmission levels in the intervals of radius $0.40 \leq r \leq 0.55$, and thus was excluded from the imperfection test.

5. Discussion and conclusions

Photonic insulation properties of silicon inverted opals have been studied for the close-to-real models including lattice disorder. Two different models of imperfection have been implemented: the normal distribution of radii and/or centre position deviations from the theoretical values and the skewed distribution experimentally determined on the huge number of colloidal particles before and after polymerization. The critical values of imperfections, which lead to the closing the bandgap, obtained from the transmission analysis in the thin films are: Imperfections in sites close the PBG when mean standard deviation $\sigma \geq 0.04$. Imperfections in radius have stronger influence, what also was noticed in the analysis of the infinite structures [10]. The PBG is closed if standard deviation $\sigma \geq 0.03$. Imperfections in both radii and positions (s&s) close the PBG with $\sigma \geq 0.02$. The second model of imperfections, when statistically imperfections obey the skewed distribution, much more affect the PBG properties than the normally distributed s&s imperfections with the closest fit $\sigma = 0.02$.

The critical values for the imperfection statistics have been proved also in the direct check of the insulating properties of the inverted opals sphere. Our calculations explicitly reveal distortion of the insulation properties of finite inverted opal structure in the presence of structural disorder characterized by as small as $\sigma = 0.01$ deviations. From multidirectional point of view radii imperfections have approximately the same influence on the PBG as site and size imperfections: both of them with $\sigma \geq 0.02$ annihilate the PBG. The most sensitive direction happens to be Γ-W, in complete accordance to the band dispersion analysis [27]. This pose a tough barrier on the level of imperfections accepted in fabrication processes.

The role of imperfections has been also tested on the transmission of PCWs. The best five designs of waveguides have been tested on their stability to possible fabrication imperfections. Two models of imperfections: randomization of the spheres radii and randomization of sizes (radii) and sites (positions) of spheres as well as two types of statistical distributions: the normal one and the skewed distribution were employed. The overall conclusion is that all waveguide designs are very sensitive to any kind of disorder. As a criterion of acceptable tolerances, the level of imperfections with $\sigma \leq 0.01$ can be recommended. This level might be softened after more advanced optimization of PCWs designs. As a new feature obtained by waveguides undergone structural randomization an appearance of new passbands beyond the PBG zone has been reported. Transmission on these frequencies is attributed to the excitation of surface modes along the distorted waveguides channels. However, the very limited applications of such bands are anticipated due to their strong overlap with the bands of the bulk inverted opal. Another interesting question, which has not been addressed here, is the influence of disorder at interfaces on transmission. For a 2D PCW disorder at the boundary layer determines actually the level of transmission through the waveguide [38]. Probably, the 3D PCWs transmission is also very sensitive for imperfections localized at the boundary, but thorough investigation of this subject is required.

Results obviously put tougher constraints on the fabrication tolerances than that obtained for the infinite structures. In general, the acceptable level of imperfections is estimated by the mean standard deviation 0.02 in case of photonic insulation by the photonic band gap effect, and 0.01 for supporting of waveguiding modes. The skewed distribution exhibits more negative effect on the PBG properties than the closest normal fit, what should be taken into account aiming polymer inverted opals for photonic applications.

Acknowledgments

We thank Manfred Stadler for excellent laboratory support. This work has been supported in part by the European Commission (EC) 6th Framework Program (FP6), under the (STREP) project NMP-4-CT-2005-017160 (NewTon).

#104159 - $15.00 USD Received 20 Nov 2008; revised 12 Dec 2008; accepted 13 Dec 2008; published 8 Jan 2009